# Optimization of Hollomon equation parameters for boron steel flow stress modeling for cold forging processes

Thanh-Cong Nguyen<sup>1</sup>, Quang-Cherng Hsu<sup>1\*</sup>, Yu-Xuan Lin<sup>1</sup>, Jing-Yuan Gao<sup>1</sup>

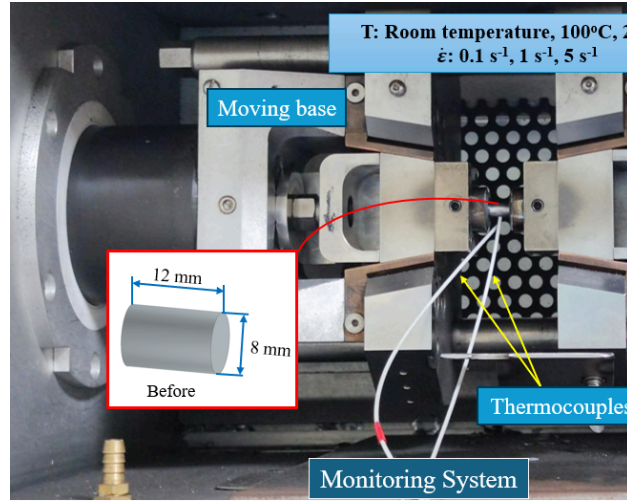
<sup>1</sup> Department of Mechanical Engineering, National Kaohsiung University of Science and Technology, 415 Chien-Kung Road, Kaohsiung 80778, Taiwan \*Corresponding author: hsuqc@nkust.edu.tw 國科會計畫編號: MOST 111-2221-E-992 -058 -MY2

## **Abstract**

This study utilized the compression test with temperature monitoring system to characterize the flow stress behavior of 10B33 boron steel under cold forging conditions. Experimental data was used to refine the Hollomon equation parameters through a Taguchi design and response surface methodology optimization. The optimized model accurately predicted compressive forces but showed limitations in temperature prediction due to the absence of an explicit temperature variable. Overall, the study successfully characterized the flow behavior of 10B33 material, offering valuable insights for cold forging process optimization.

**Keywords:** boron steel, flow stress, Hollomon equation, optimization, response surface methodology, finite element analysis.

# 1. Introduction



AISI 10B33, a medium-carbon steel alloyed with boron, exhibits notable strength and has garnered extensive application across diverse industries. The incorporation of boron, even in small amounts (0.002 to 0.005 weight percent), significantly enhances the

Table 1. Chemical composition of 1

Element		Figure . The c	compression expe
%wt	0.32~0.36	0.15~0.35	0.70~1.00

steel's hardenability, enabling it to attain elevated hardness levels through heat treatment [1]. Consequently, AISI 10B33 emerges as a compelling material choice when high strength is imperative, finding frequent use in automotive and construction components, fasteners, and various other applications [2]. In the realm of industrial metal forming processes like forging and extrusion, the accurate prediction of flow stress is paramount for ensuring effective process design. Constitutive models provide a mathematical framework for this prediction, establishing a relationship between flow stress and deformation while accounting for crucial variables such as temperature, strain rate, and strain [3]. The investigation and modeling of flow stress in steel materials have long been a research interest focus, driving advancements in various industries [4-7]. The flow stress, a measure of a material's resistance to deformation under applied stress, is a critical parameter in understanding and

# 中華民國114年11月17日

optimizing metal forming processes, such as forging, extrusion, and rolling. Accurate flow stress prediction enables engineers to design efficient and cost-effective manufacturing processes, ensuring the production of high-quality components with desired mechanical properties. Recent studies have mainly focused on studying the properties of boron steels at high temperatures. Li et al. [8] address the challenge of accurate constitutive behavior identification in hot stamping of boron steel, a complex process involving thermal-mechanical coupling and transformation. They introduce a novel grip design to regulate the Uniform Temperature Zone (UTZ) in Gleeble tensile tests and develop a robust DIC system for precise strain calibration at high temperatures and strain rates. Their research highlights the importance of accurate strain measurement and appropriate UTZ length for reliable parameter identification, ultimately enhancing hot stamping simulation accuracy. Zhou et al. [9] investigated the thermo-mechanical behavior of 22MnB5 boron steel, a material crucial for lightweight vehicle manufacturing, through thermal tensile tests across a wide range of temperatures and strain rates. The study focused on understanding the correlation between thermoforming process parameters and the resulting microstructure, which ultimately dictates the mechanical properties of the formed components. A modified Arrhenius-type constitutive model was developed to accurately predict flow stress behavior, contributing to improved process optimization and component design in hot stamping applications. Tricarico [10] Palmieri and investigated the deformation behavior and constitutive description of two quenchable boron steels (USIBOR®1500 and USIBOR®2000) relevant to the Press Hardening process. Hot tensile tests were conducted under various temperatures and strain rates, and an Arrhenius-type equation was employed to model the material constitutive behavior. The model's validity was confirmed by comparing experimental and predicted data, demonstrating its effectiveness for both steels. Zhang et al. [11] conducted a study to evaluate the impact of temperature gradients, a common occurrence in Gleeble tensile tests of boron steel under hot stamping conditions, on the accuracy of measured material properties. By employing digital image correlation and varying gauge lengths, they observed a bell-shaped strain distribution and gauge length-dependent variations in strain, stress-strain curves, fracture strains, and flow stresses. Li et al. [12] studied the constitutive relationship of boron steel B1500HS under various microstructures deformation conditions. Through isothermal uniaxial tension tests and regression analysis, they developed

constitutive equations based on modified Arrhenius and Johnson-Cook models to describe the flow stress behavior of the steel during hot deformation. The accuracy of these models was validated by comparing computational and experimental data, demonstrating their effectiveness in predicting material response. While recent research has extensively explored the high-temperature deformation of boron steels, there remains a lack of comprehensive investigation into modeling the flow stress of boron steel at or near room temperature. This is significant as accurate flow stress prediction is essential for optimizing cold forging processes and ensuring the quality of the final products. This study aims to investigate and establish a best-fit model for spheroidized AISI 10B33 boron-alloyed steel in cold forging, thereby contributing to a deeper understanding of deformation behavior under varying processing conditions. The chemical composition of 10B33 used in this study is presented in Table 1.

# 2. Research methodology

The Gleeble test, a versatile thermal-mechanical simulator, has become an indispensable tool for characterizing the deformation behavior of materials under various conditions. In the context of cold forging, the Gleeble test offers a controlled and repeatable environment to investigate the flow stress response of boron steel at different strain rates and temperatures. By subjecting samples to compressive deformation at relevant process parameters, the Gleeble test provides valuable data for material modeling and process optimization. Figure 1 depicts the compression testing system used in this study.

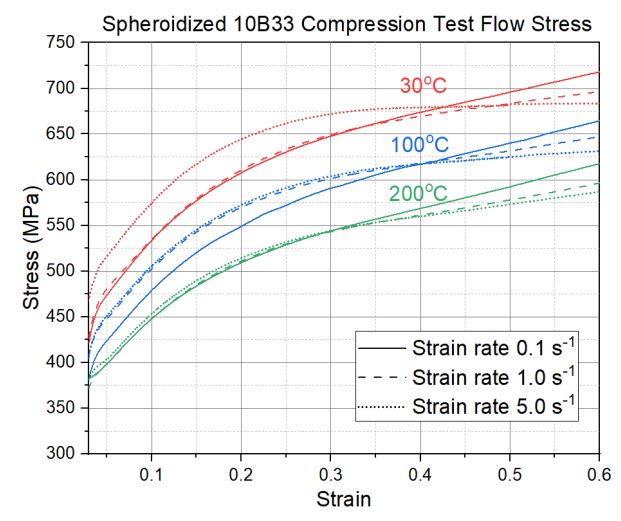


Figure 2. Compression experiment flow curve

This study aims to employ the Gleeble test to experimentally determine the flow stress behavior of

# 中華民國114年11月17日

boron steel at and near room temperature conditions (including room temperature, 100°C and 200°C).

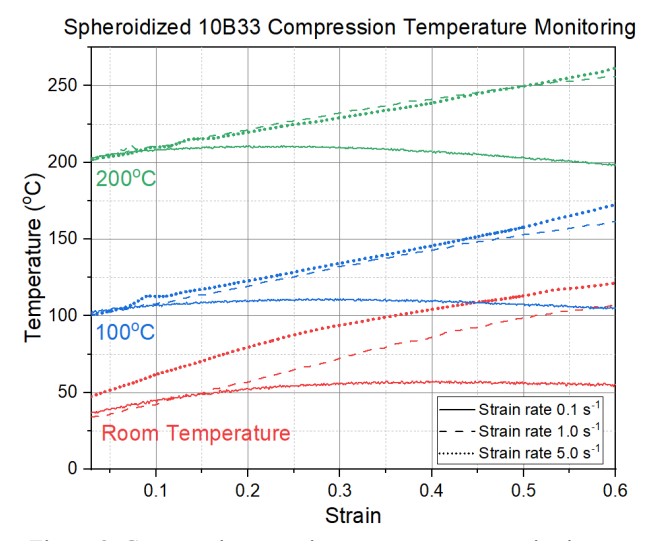


Figure 3. Compression experiment temperature monitoring

The obtained data will be utilized to refine the Hollomon equation parameters and validate the optimized model developed in the further section. Accurate modeling of flow stress is crucial for predicting the deformation behavior and optimizing the process parameters in cold forging operations. The Hollomon equation, a widely used empirical model, has been extensively employed for this purpose. In utilizing the Hollomon equation, which presupposes uniform deformation, the true strain and true stress were derived from the displacement and load data acquired during the compression test. This involved employing Equations (1) and (2):

$$\varepsilon = \int_{h_0}^{h} \frac{1}{h} \, dh = \ln\left(\frac{h}{h_0}\right) \tag{1}$$

$$\sigma = \frac{P}{A} = \frac{Ph}{A_0 h_0} \tag{2}$$

wherein P is the applied force, h represents the instantaneous height of the cylindrical sample during compression,  $h_0$  denotes the initial height of the cylinder, and  $A_0$  signifies the pre-deformation diameter of the specimen [13]. Subsequently, the computed strain-stress relationship was expressed with strength coefficient (k) and strength hardening (n), as delineated in Equation (3):

$$\sigma = k\varepsilon^n \tag{3}$$

In this study, the flow curve at a strain rate of 1 s<sup>-1</sup> and a temperature of 100°C was utilized. Upon obtaining the Hollomon equation model under these conditions, it

was observed that the model's predictions deviated significantly from experimental results, particularly at larger strains. Consequently, subsequent analyses focused on optimizing the parameters k and n to achieve the best-fit flow curve. Noting that the model's predicted curve tended to overestimate stress at higher strains, a Taguchi experimental design was employed.

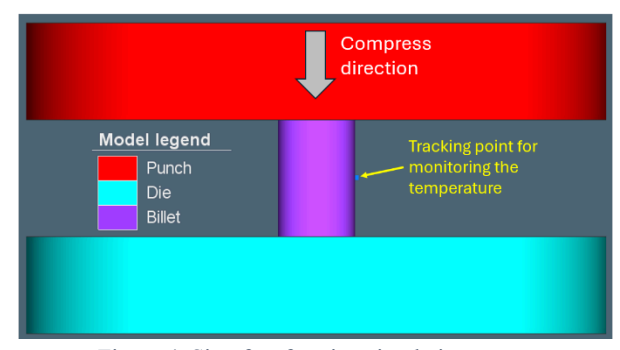


Figure 4. Simufact forming simulation setup

The k and n values derived from the initial experiment were designated as the highest level (coded as +1), with subsequent levels (coded as 0 and -1) representing 10% decrements from this baseline. Each experiment corresponded to a unique combination of k and n, resulting in a distinct stress curve. These stress curves were then input as material parameters for finite element simulations in Simufact forming (as described in Figure 4). The maximum extrusion force and the maximum temperature at the thermocouple location were extracted from the simulation results. Regression analysis was employed to establish a relationship between these output factors and the parameters k and n. Subsequently, response surface methodology was utilized to optimize k and n, aiming to minimize the discrepancy between simulated and experimental values for maximum extrusion force and temperature. This process is referred to as multi-objective optimization, where multiple goals (in this case, approaching both extrusion force and temperature to the target value) are considered simultaneously.

# 第十二屆台灣塑性加工研討會論文集

# 中華民國114年11月17日

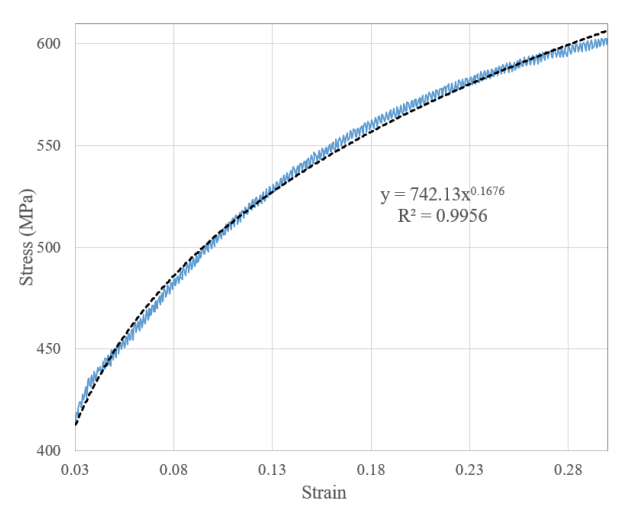


Figure 5. Fitting equation at strain rate 1s<sup>-1</sup> and 100°C

In analyzing the compression test data presented in Figure 2, two distinct trends are discernible. Firstly, flow stress exhibits an inverse relationship with the initial set temperature, decreasing as the latter rises. Secondly, a more pronounced decline in flow stress is observed at higher strain rates compared to lower ones. This phenomenon can be elucidated by examining the temperature fluctuations during the test, as depicted in Figure 3. The general trend reveals a positive correlation between strain rate and the temperature differential from the initial value, indicating material softening induced by deformation-generated heat. Consequently, to minimize the influence temperature on the flow curve, the strain region between 0.03 and 0.3 was selected for formulating the Hollomon equation.

# 3. Results and Discussions

# 3.1 Hollomon model

After extracting the data from strain 0.03 to 0.3, curve fitting method was used to find the suitable expression. Figure 5 shows that the coefficient strength and hardening strength at strain rate 1s<sup>-1</sup> and 100°C are 742.13 and 0.1676, respectively, as shown in equation (4).

$$\sigma = k\varepsilon^n = 742.13\varepsilon^{0.1676} \tag{4}$$

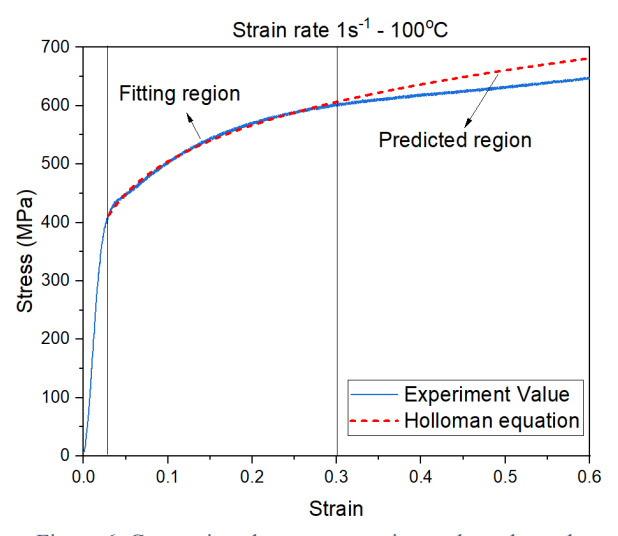


Figure 6. Comparison between experimental results and Hollomon equation modelling at strain rate 1s<sup>-1</sup> - 100°C

The stress-strain curve of 10B33 spheroidizing steel at a strain rate of 1 s<sup>-1</sup> and 100°C reveals a characteristic flow stress behavior (as shown in Figure 6), with an initial elastic region followed by plastic deformation. The Hollomon equation effectively models the material's behavior within the strain range of 0.03 to 0.3, demonstrating a power-law relationship. However, at higher strains, the model overestimates stress, suggesting the influence of factors such as strain hardening and deformation-induced heating. This discrepancy underscores the necessity for more sophisticated models or modifications to the Hollomon equation to comprehensively capture the material's response across the whole range of strain.

# 3.2 Model parameter optimizing

The Taguchi design levels were computed and are summarized in Table 2. This yielded nine distinct combinations of k and n, each corresponding to a unique flow curve. Subsequently, this data was incorporated into the Simufact forming software database to facilitate compression simulations. Table 3 presents a comprehensive overview of these k and n combinations alongside the corresponding simulation outcomes, specifically the maximum extrusion force and temperature observed at the designated tracking point.

Table 2. Levels of Taguchi design

Level	-1	0	+1
k	607.19	674.66	742.13
n	0.1371	0.1523	0.1676

# 第十二屆台灣塑性加工研討會論文集

# 中華民國114年11月17日

Table 3. Design of experiments and simulation results

Run no.	k	n	Max. Force (kgf)	Max. Temp. (°C)
1	607.19	0.1371	5572	166.6
2	607.19	0.1523	5522	165.5
3	607.19	0.1676	5528	164.4
4	674.66	0.1371	6260	173.5
5	674.66	0.1523	6209	172.3
6	674.66	0.1676	6141	171.2
7	742.13	0.1371	7037	180.3
8	742.13	0.1523	6807	173.1
9	742.13	0.1676	6764	177.9
Expe	riment/Targ	et value	6307.4	163

Figures 7 and 8 present the results of response surface methodology analyses using coded coefficients, for maximum force and temperature respectively. The models demonstrate strong explanatory power, accounting for 99.85% and 93.27% of the variation in their respective response variables. The linear terms (k and n) emerge as the most influential factors, whereas the squared and interaction terms exhibit less significance. Overall, the models demonstrate a good fit to the data, suggesting their capability in providing reliable predictions based on the predictor variables.

# **Coded Coefficients**

Term	Coef	SE Coef	T-Value	P-Value	VIF
Constant	6178.0	27.5	224.26	0.000	
k	664.3	15.1	44.02	0.000	1.00
n	-72.7	15.1	-4.82	0.017	1.00
k*k	1.7	26.1	0.06	0.953	1.00
n*n	37.9	26.1	1.45	0.243	1.00
k*n	-57.2	18.5	-3.10	0.053	1.00

# **Model Summary**

S	R-sq	R-sq(adj)	R-sq(pred)
36.9593	99.85%	99.60%	98.53%

# **Analysis of Variance**

Source	DF	Adj SS	Adj MS	F-Value	P-Value
Model	5	2695652	539130	394.68	0.000
Linear	2	2679212	1339606	980.69	0.000
k	1	2647529	2647529	1938.18	0.000
n	1	31683	31683	23.19	0.017
Square	2	2879	1440	1.05	0.450
k*k	1	6	6	0.00	0.953
n*n	1	2874	2874	2.10	0.243
2-Way Interaction	1	13094	13094	9.59	0.053
k*n	1	13094	13094	9.59	0.053
Error	3	4098	1366		
Total	8	2699750			

Figure 7. Response surface regression of maximum force (F) versus k and n

# **Coded Coefficients**

Term	Coef	SE Coef	T-Value	P-Value	VIF
Constant	170.99	1.71	99.74	0.000	
k	5.800	0.939	6.18	0.009	1.00
n	-1.150	0.939	-1.22	0.308	1.00
k*k	-1.03	1.63	-0.64	0.570	1.00
n*n	2.02	1.63	1.24	0.302	1.00
k*n	-0.05	1.15	-0.04	0.970	1.00

# **Model Summary**

S	R-sq	R-sq(adj)	R-sq(pred)
2.29993	93.27%	82.06%	25.79%

# **Analysis of Variance**

Source	DF	Adj SS	Adj MS	F-Value	P-Value
Model	5	220.053	44.011	8.32	0.056
Linear	2	209.771	104.886	19.83	0.019
k	1	201.836	201.836	38.16	0.009
n	1	7.935	7.935	1.50	0.308
Square	2	10.300	5.150	0.97	0.472
k*k	1	2.136	2.136	0.40	0.570
n*n	1	8.164	8.164	1.54	0.302
2-Way Interaction	1	0.009	0.009	0.00	0.970
k*n	1	0.009	0.009	0.00	0.970
Error	3	15.869	5.290		
Total	8	235.922			

Figure 8. Response surface regression of maximum temperature at tracking point (T) versus k and n

# 第十二屆台灣塑性加工研討會論文集

# 中華民國114年11月17日

$$F = -1504 + 17.82k - 16913n + 0.00037k^{2} + 162990n^{2} - 55.6kn$$
 (5)

$$T = 218 + 0.399k - 2692n + 0.000227k^{2} + 8688n^{2} - 0.05kn$$
 (6)

The optimization results indicate that a k value of 688.6 and an n value of 0.154044 yield the closest approximation to the targeted T and F values of 163 and 6307.4, respectively. This solution, visually represented in Figures 9 and 10, achieves a composite desirability of 0.690726, signifying a satisfactory compromise between the two objectives. The optimized Hollomon model, as presented in Equation 7, was subsequently employed in simulations.

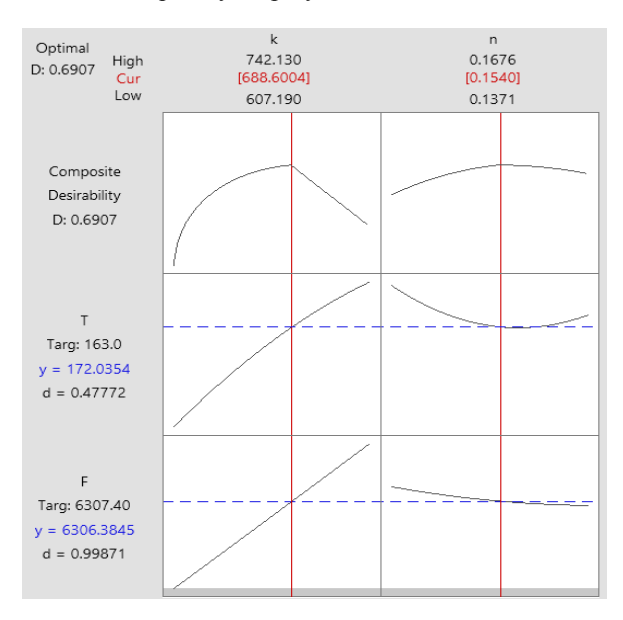


Figure 9. RSM optimizing based on calculated results

#### **Parameters**

Response	Goal	Lower	Target	Upper	Weight	Importance
T	Target	146.7	163.0	180.3	1	1
F	Target	5522.0	6307.4	7037.0	1	1

#### Solution

			T	F	Composite
Solution	k	n	Fit	Fit	Desirability
1	688.600	0.154044	172.035	6306.38	0.690726

# **Multiple Response Prediction**

Variable	Setting			
k	688.6			
n	0.154044			
Response	Fit	SE Fit	95% CI	95% PI
Response T	Fit 172.04		95% CI (166.71, 177.36)	

Figure 10.RSM optimization results

$$\sigma = K \varepsilon^n = 688.6 \varepsilon^{0.154044}$$
 (7)

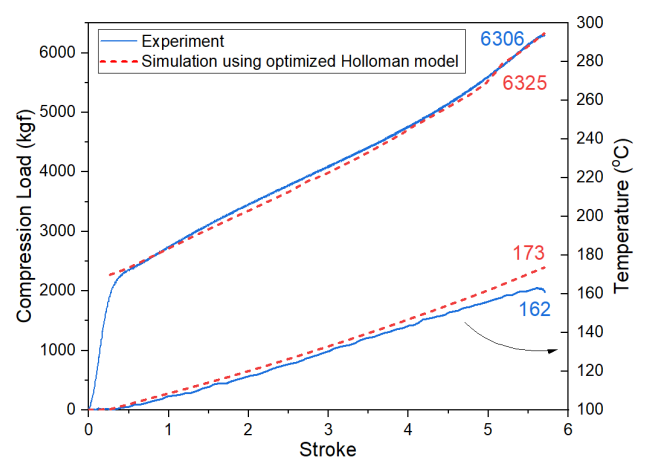


Figure 11. Comparison between experiment and simulation using optimal Hollomon model at strain rate 1s<sup>-1</sup> and 100°C

Figure 11 demonstrates a high degree of concordance between the simulated and experimental compressive forces, with a deviation of less than 1%. However, a discrepancy of up to 10 degrees Celsius (exceeding 6%) was noted in the temperature prediction. This underscores a limitation of the current approach, wherein the model lacks an explicit temperature variable. Nevertheless, the study successfully characterizes the flow behavior of 10B33 material under cold forging conditions.

# 4. Conclusions

conclusion, this In study successfully characterized the flow behavior of 10B33 material under cold forging conditions by optimizing the Hollomon equation parameters using a combination of experimental data, Taguchi design, and response surface methodology. Despite the model's limitations in accurately predicting temperature, the high degree of agreement between simulated and experimental compressive forces validates its efficacy representing the material's flow stress behavior. This research provides valuable insights for optimizing cold forging processes and enhancing the accuracy of numerical simulations. Future work may focus on incorporating temperature dependence into the model for improved predictive capabilities across a wider range of process conditions.

# 5. References

- [1]. Campbell, J. (2020). The Mechanisms of Metallurgical Failure-the Origin of Fracture DOI: 10.1016. B978-0-12-822411-3.00001-0.
- [2]. Kong, H., Chao, Q., Rolfe, B., & Beladi, H. (2019). One-step quenching and partitioning treatment of a

# 中華民國114年11月17日

- tailor welded blank of boron and TRIP steels for automotive applications. *Materials & Design*, 174, 107799.
- [3]. Ottosen, N. S., & Ristinmaa, M. (2005). *The mechanics of constitutive modeling*. Elsevier.
- [4]. Lee, H. W., Yoo, J. H., Kwon, Y. C., & Kang, J. H. (2021). Calculation Method for Cold Flow Stress of Al6082 Based on Tensile Test and Compression Test Results. *International Journal of Precision Engineering and Manufacturing*, 22(8), 1337-1344.
- [5]. Deb, S., Muraleedharan, A., Immanuel, R. J., Panigrahi, S. K., Racineux, G., & Marya, S. (2022). Establishing flow stress behaviour of Ti-6Al-4V alloy and development of constitutive models using Johnson-Cook method and Artificial Neural Network for quasi-static and dynamic loading. Theoretical and Applied Fracture Mechanics, 119, 103338.
- [6]. Nahrmann, M., & Matzenmiller, A. (2021). A critical review and assessment of different thermoviscoplastic material models for simultaneous hot/cold forging analysis. international journal of material forming, 14, 641-662.
- [7]. Şimşir, C., & Duran, D. (2018). A flow stress model for steel in cold forging process range and the associated method for parameter identification. The International Journal of Advanced Manufacturing Technology, 94, 3795-3808.
- [8]. Li, Y., Li, S., Chen, Y., & Han, G. (2019). Constitutive parameters identification based on DIC assisted thermo-mechanical tensile test for hot stamping of boron steel. *Journal of Materials Processing Technology*, 271, 429-443.
- [9]. Zhou, Q., Guo, P., & Qin, F. (2022). Stress response behavior, microstructure evolution and constitutive modeling of 22MnB5 boron steel under isothermal tensile load. *Metals*, *12*(6), 930.
- [10]. Palmieri, M. E., & Tricarico, L. (2022). Comparison of flow behaviors at high temperature of two press hardening boron steels with different hardenability. *Metals*, 12(11), 1935.
- [11]. Zhang, R., Shao, Z., Lin, J., & Dean, T. A. (2020). Measurement and analysis of heterogeneous strain fields in uniaxial tensile tests for boron steel under hot stamping conditions. *Experimental Mechanics*, 60, 1289-1300.
- [12]. Li, H., He, L., Zhao, G., & Zhang, L. (2013). Constitutive relationships of hot stamping boron steel B1500HS based on the modified Arrhenius and Johnson–Cook model. *Materials Science and Engineering: A*, 580, 330-348.

[13]. Hosford, W. F., & Caddell, R. M. (2011). *Metal forming: mechanics and metallurgy*. Cambridge University Press.